

# Curie and Néel Temperatures of Quantum Magnets

**J. Oitmaa and Weihong Zheng**

School of Physics, The University of New South Wales, Sydney, NSW 2052, Australia

**Abstract.** We estimate, using high-temperature series expansions, the transition temperatures of the spin  $\frac{1}{2}$ , 1 and  $\frac{3}{2}$  Heisenberg ferromagnet and antiferromagnet in 3-dimensions. The manner in which the difference between Curie and Néel temperatures vanishes with increasing spin quantum number is investigated.

It is well known that in classical spin models, such as the Ising or classical Heisenberg models, on bipartite lattices the critical temperature (if it exists) is the same for ferromagnetic exchange (Curie temperature) as for antiferromagnetic exchange (Néel temperature). This is a direct consequence of the free energy being an even function of the exchange parameter  $J$ . It has also been known for some time, but perhaps less widely, that for the quantum spin- $\frac{1}{2}$  Heisenberg model the Curie and Néel temperatures are unequal. Early work [1, 2] put the Néel temperature some 10% above the Curie temperature for spin- $\frac{1}{2}$ , for both the simple cubic (SC) and body-centred cubic (BCC) lattices, with the difference decreasing rapidly with increasing  $S$ . However these results were based on rather short series (six terms) and the critical point estimates contained large uncertainties.

We have re-investigated this question, using substantially longer series (14th order for  $S = \frac{1}{2}$ , 12th order for  $S = 1$ , 9th order for  $S = \frac{3}{2}$ ). This is made possible not only by the massive increase in computing power now available, but also by the development of efficient linked-cluster expansion methods. The reader is referred to a recent review [3] for further details of this method.

The Hamiltonian is written in the form

$$H = -J \sum_{\langle ij \rangle} \mathbf{S}_i \cdot \mathbf{S}_j - h \sum_i S_i^z - h_s \sum_i \eta_i S_i^z \quad (1)$$

where the  $\mathbf{S}_i$  are spin- $S$  operators,  $h$  and  $h_s$  are uniform and staggered fields, with  $\eta_i = \pm 1$  on respective sublattices, and the interaction is taken between nearest neighbours  $\langle ij \rangle$ .  $J > 0$  ( $< 0$ ) corresponds to the ferromagnet (antiferromagnet). While (1) contains the form of the exchange energy for a real spin- $S$  system, for comparison between different  $S$ -values and, in particular, for passage to the classical limit  $S \rightarrow \infty$ , it is convenient to write  $\tilde{J} = JS(S+1)$  and to express critical temperatures in units of  $\tilde{J}/k_B$ .

The critical temperature  $k_B T_c/J$  is most reliably obtained from the strongly divergent ‘ordering’ susceptibility in zero field: the uniform susceptibility  $\chi$  for the ferromagnet or the staggered susceptibility  $\chi_s$  for the antiferromagnet. High-temperature series for these quantities can be derived in the form

$$\chi, \chi_s = \sum_{r=0}^{\infty} a_r K^r \quad (2)$$

where  $K = |J|/k_B T$  and the  $a_r$  are numerical coefficients. The uniform susceptibility for the spin- $\frac{1}{2}$  case is known through order  $K^{14}$  [4], for both the SC and BCC lattices. In the present paper we give the staggered susceptibility series to the same order. This represents an addition of six new terms to the previously known series[5]. At the same time we compute uniform and staggered susceptibilities for the  $S = 1$  case, through order  $K^{12}$  and  $K^{11}$  respectively, for both lattices, extending the previous series by five terms. We have also calculated the corresponding series for  $S = \frac{3}{2}$  through order  $K^9$ . For the classical  $S = \infty$  model the susceptibility series is known through  $K^{21}$ [6] and we will use this series in our comparison.

Tables 1, 3 and 2 list the series coefficients, in integer format, for both the SC and BCC lattices. The coefficients are positive and appear to be quite regular, suggesting that the radius of convergence is determined by the physical singularity on the positive real axis (we will return to this point later!) Closer inspection, however, reveals some oscillation, reflecting interference from non-physical singularities near the circle of convergence. Although we do not base our analysis on this, it is instructive to see a ratio plot[7]. We show such a plot in Figure 1. Looking at the SC lattice first, it is evident that the  $S = \frac{1}{2}$  series, in particular, shows a strong 4-term oscillation. This results from a pair of singularities on, or near, the imaginary axis, near the circle of convergence. The  $S = 1$  series are much more regular and, qualitatively, look quite similar to the  $S = \infty$  case. The BCC series are rather regular, even for  $S = \frac{1}{2}$ . There is a 2-term oscillation in all series, which is characteristic of bipartite lattices. Apart from the  $S = \frac{1}{2}$  (SC) case, reasonable estimates of the Curie and Néel temperatures can be made visually. Unless something totally unexpected were to occur at higher orders, it seems clear that the Néel temperature exceeds the Curie temperature for both  $S = \frac{1}{2}$  and  $S = 1$  (remembering that the intercept on the ordinate axis is  $k_B T_c / \tilde{J}$ ). The very similar limiting slope of the different plots is consistent with the universality expectation that all quantities diverge with the same exponent  $\gamma$ .

To obtain more accurate estimates of the critical parameters we turn to Padé approximants[7]. Tables 4, 5 give estimates of the critical point  $K_C$  and exponent  $\gamma$ , assuming a normal power-law singularity

$$\chi, \chi_s \sim C_0(1 - K/K_C)^{-\gamma}; \quad K \rightarrow K_C - \quad (3)$$

obtained from high-order Padé approximants to the logarithmic derivative series. Different approximants give quite consistent results and we summarize the overall estimates of the critical temperature in Table 6. The exponent estimates from the highest approximants are around 1.42 ( $S = \frac{1}{2}$ ), 1.41 ( $S = 1$ ). Early studies of the  $S = \infty$  series also gave values in this range, although the recent long series give lower values, approaching the field theory prediction  $\gamma \simeq 1.39$ . Our results are consistent with the universality expectation.

Figure 2 shows plots of critical temperatures  $k_B T_c / S(S+1)J$  versus  $1/S(S+1)$ . The plots appear linear, particularly if the  $S = \frac{1}{2}$  points are excluded, and indicate that, to a very good approximation

$$k_B T_c / J \sim aS(S+1) + b \quad (4)$$

where  $a, b$  are constants independent of  $S$ . Their values are

	SC		BCC	
	$\chi$	$\chi_s$	$\chi$	$\chi_s$
$a$	1.4429		2.0542	
$b$	-0.288	-0.150	-0.320	-0.174

This linear relation may then be used to obtain reliable estimates of Curie and Néel temperature for values  $S > \frac{3}{2}$ .

With our longer series we are also able, for the first time, to estimate values for the amplitudes  $C_0$  of the leading singular term (3). This is done in two ways. The first is to use the estimates of  $K_C$ ,  $\gamma$  obtained previously, form the series for

$$(1 - K/K_C)^\gamma \chi \sim C_0 + \dots; \quad K \rightarrow K_C - \quad (5)$$

and evaluate Padé approximants to this series at  $K_C$ . The second is to compute the series for

$$\chi^{1/\gamma} = C_0^{1/\gamma} (1 - K/K_C)^{-1} \quad (6)$$

Padé approximants to this series should have a simple pole at  $K_C$  with residue  $K_C C_0^{1/\gamma}$ . Both methods give consistent results. We give in Table 6 our best estimates and error. As usual with series analysis, these are not true statistical errors but only confidence limits based on the spread of results. As can be seen from Table 6, these amplitudes are all of order 1 and show a decrease of some 30% on going from  $S = \frac{1}{2}$  to  $S = \infty$ , with the antiferromagnetic amplitude some 5% smaller than the ferromagnetic one.

The conclusion that the Curie temperature  $T_C$  is lower than the Néel temperature  $T_N$  has a puzzling consequence, as has been remarked on before [2]. Assuming that the ferromagnetic susceptibility  $\chi(K)$  also has a weak, energy like singularity at  $-K_N$  ( $K_N < K_C$ ), as is known to be the case for the Ising model, means that the radius of convergence of the series is  $|K_N|$ . Hence the series coefficients must, at some point, begin to alternate in sign. To check this point further we follow the procedure of Baker *et al.*[8], in seeking evidence for a singularity at  $-K_N$  in the uniform susceptibility, and at  $-K_C$  in the staggered susceptibility. To this end we form the series for

$$F(K) = \frac{d}{dK} \left( \frac{d}{dK} \ln \chi(K) - \frac{\gamma}{K_C - K} \right) \quad (7)$$

and

$$F_s(K) = \frac{d}{dK} \left( \frac{d}{dK} \ln \chi_s(K) - \frac{\gamma}{K_N - K} \right) \quad (8)$$

The first step subtracts out the dominant physical singularity from the logarithmic derivative series. This series is expected to have a weak singularity at the corresponding Néel or Curie point. The final differentiation is to strengthen this singularity. In Table 7 we show estimates of the location of this secondary singularity and the corresponding residue for the  $S = \frac{1}{2}$  series on the BCC lattice. As is clear, the series  $F(K)$  shows a consistent pole at  $K \simeq -0.72$ , consistent with the direct estimate of  $K_N$  (Table 4). Similarly the series  $F_s(K)$  shows a consistent pole at  $K \simeq -0.799$ , consistent with the direct estimate of  $K_C$  (Table 4). These numerical estimates will, of course, depend on the choice made for  $K_C$ ,  $K_N$ ,  $\gamma$  in Eqs. (7) and (8), but are found to be relatively insensitive to this choice. We have not repeated this analysis for the SC case or for  $S = 1, \frac{3}{2}$ .

**Table 1.** Series for  $\chi$  and  $\chi_s$  for spin- $\frac{1}{2}$ . To avoid fractions a multiplier  $4^{n+1}n!$  for  $\chi$ , or  $4^{n+1}(n+1)!$  for  $\chi_s$  has been used, where  $n$  is the power of  $K$ .

n	$\chi$	$\chi_s$
Simple Cubic Lattice $S = \frac{1}{2}$		
0	1	1
1	6	12
2	48	168
3	528	2880
4	7920	59376
5	149856	1478592
6	3169248	42357024
7	77046528	1353271296
8	2231209728	48089027328
9	71938507776	1908863705088
10	2446325534208	83357870602752
11	92886269386752	3926123179720704
12	3995799894239232	198436560561973248
13	180512165153832960	10823888709015846912
14	8443006907441565696	635114442481347244032
Body Centred Cubic Lattice $S = \frac{1}{2}$		
0	1	1
1	8	16
2	96	320
3	1664	8192
4	36800	248768
5	1008768	8919296
6	32626560	367854720
7	1221399040	17216475136
8	51734584320	899434884096
9	2459086364672	51925815320576
10	129082499311616	3280345760086016
11	7432690738003968	225270705859919872
12	464885622793134080	16704037174526894080
13	31456185663820136448	1330557135528577925120
14	2284815238218471260160	113282648639921512955904

## References

- [1] Rushbrooke G S and Wood P J 1963 *Mol Phys* **6**, 409.
- [2] Rushbrooke G S, Baker G A Jr and Wood P J 1974 *Phase Transitions and Critical Phenomena* Vol. 4 (Academic Press, New York).
- [3] Gelfand M P and Singh R R P 2000 *Adv Phys* **49**, 93.
- [4] Oitmaa J and Bornilla E 1996 *Phys. Rev. B* **53**, 14228.
- [5] Pan K K 1999 *Phys. Rev. B* **56**, 1168.
- [6] Butera P and Comi M 1997 *Phys Rev B* **56**, 8212.
- [7] Guttman A J 1989 *Phase Transitions and Critical Phenomena* Vol. 13 (Academic Press, , New York).
- [8] Baker G A Jr, Gilbert H E, Eve J & Rushbrooke G S 1967, *Phys Rev* **164**, 800.

**Table 2.** Series for  $\chi$  and  $\chi_s$  for spin-1. To avoid fractions a multiplier  $3^{n+1}n!/2$  ( $3^{n+1}(n+1)!/2$ ) has been used for  $\chi$  ( $\chi_s$ ) series, where  $n$  is the power of  $K$ .

n	$\chi$	$\chi_s$
Simple Cubic Lattice $S = 1$		
0	1	1
1	12	24
2	222	702
3	5904	26280
4	201870	1184526
5	8556912	63357984
6	426905802	3887604666
7	24674144724	270348199128
8	1616505223518	20988390679758
9	118701556096392	1802403961243776
10	9628527879611262	169418364565523958
11	856813238084411136	17314303199655636792
12	82856991914713902402	
Body Centred Cubic Lattice $S = 1$		
0	1	1
1	16	32
2	424	1320
3	16512	71136
4	819240	4588968
5	50363136	351263232
6	3652143480	30873601080
7	307454670000	3082065903648
8	29310549057000	343320789071016
9	3133368921937824	42320100429654912
10	370060173560963304	5709664512091086984
11	47968071364509850944	837942419330764322976
12	6756542767252059234840	

**Table 3.** Series for  $\chi$  and  $\chi_s$  for spin- $\frac{3}{2}$ . To avoid fractions a multiplier  $2^{n+2}n!/5$  ( $2^{n+3}(n+1)!/5$ ) has been used for  $\chi$  ( $\chi_s$ ) series, where  $n$  is the power of  $K$ .

n	$\chi$	$\chi_s$
Simple Cubic Lattice $S = \frac{3}{2}$		
0	1	2
1	60	60
2	1440	2220
3	50136	106032
4	2241660	6103230
5	124125372	417121164
6	8102868414	32715943017
7	613292153184	2911926450048
8	52599376466556	289263779556198
9	5056198898505288	31792485934519488
Body Centred Cubic Lattice $S = \frac{3}{2}$		
0	1	2
1	80	80
2	2720	4160
3	136448	283776
4	8751600	23240440
5	696028496	2263139152
6	65331028472	253095247076
7	7121212898544	32175304799424
8	879298191968624	4563926306507096
9	121768840349153216	716734730963510496

**Table 4.** Estimates of critical point  $K_C$  and exponent  $\gamma$  (in brackets) from  $[N, D]$  Padé approximants to the spin- $\frac{1}{2}$  uniform/staggered susceptibility series. Defective PA's are denoted \*.

Spin $S = \frac{1}{2}$				
$[N, D]$	Simple Cubic		Body Centred Cubic	
	F ( $\chi$ )	AF ( $\chi_s$ )	F ( $\chi$ )	AF ( $\chi_s$ )
[6, 7]	1.1900 (1.414)	1.0577 (1.426)	0.7935 (1.416)	0.7266 (1.436)
[7, 6]	1.1925 (1.432)	1.0611 (1.455)	0.7935 (1.416)	0.7266 (1.435)
[5, 7]	1.1914 (1.421)	1.0598 (1.440)	0.7937 (1.419)	0.7266 (1.434)
[6, 6]	1.1914 (1.421)	1.0597 (1.439)	0.7936 (1.417)	0.7264 (1.431)
[7, 5]	1.1931 (1.438)	*	0.7939 (1.423)	0.7267 (1.436)
[5, 6]	1.1910 (1.418)	1.0592 (1.434)	0.7937 (1.418)	0.7264 (1.432)
[6, 5]	1.1901 (1.411)	1.0583 (1.425)	0.7936 (1.418)	0.7264 (1.432)

**Table 5.** Estimates of critical point  $K_C$  and exponent  $\gamma$  (in brackets) from  $[N, D]$  Padé approximants to the Spin-1 uniform/staggered susceptibility series. Defective PA's are denoted \*.

Spin $S = 1$				
Simple Cubic		Body Centred Cubic		
$[N, D]$	F ( $\chi$ )	AF ( $\chi_s$ )	F ( $\chi$ )	AF ( $\chi_s$ )
[5, 6]	0.38478 (1.409)		0.26400 (1.404)	
[6, 5]	0.38478 (1.409)		0.26398 (1.403)	
[4, 6]	0.38478 (1.409)	*	0.26397 (1.403)	0.25431 (1.405)
[5, 5]	0.38475 (1.408)	*	0.26389 (1.398)	0.25431 (1.401)
[6, 4]	0.38467 (1.406)	0.36541 (1.409)	*	0.25410 (1.395)
[4, 5]	0.38487 (1.411)	0.36566 (1.417)	*	0.25410 (1.395)
[5, 4]	0.38483 (1.410)	0.36565 (1.417)	*	0.25396 (1.390)

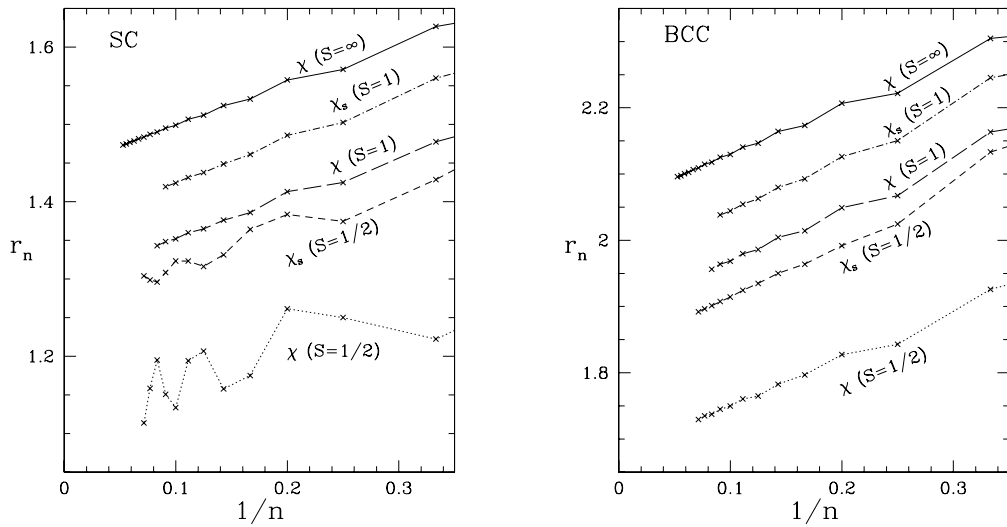
**Table 6.** Estimates of the critical temperatures and leading susceptibility amplitudes, from Padé approximant analysis.

SC Lattice							
	$S = \frac{1}{2}$		$S = 1$		$S = \frac{3}{2}$		$S = \infty$
	F ( $\chi$ )	AF ( $\chi_s$ )	F ( $\chi$ )	AF ( $\chi_s$ )	F ( $\chi$ )	AF ( $\chi_s$ )	$\chi$
$K_C$	1.192(2)	1.059(2)	0.38478(15)	0.3656(2)	0.195(3)	0.190(1)	0.69304
$k_B T_c / J$	0.839(1)	0.944(2)	2.599(1)	2.735(1)	5.13(8)	5.26(3)	
$k_B T_c / \tilde{J}$	1.119(2)	1.259(2)	1.2994(5)	1.3676(7)	1.37(2)	1.404(7)	1.4429
$C_0$	1.26(2)	1.20(3)	1.11(2)	1.07(4)			0.9030
BCC Lattice							
	$S = \frac{1}{2}$		$S = 1$		$S = \frac{3}{2}$		$S = \infty$
	F ( $\chi$ )	AF ( $\chi_s$ )	F ( $\chi$ )	AF ( $\chi_s$ )	F ( $\chi$ )	AF ( $\chi_s$ )	$\chi$
$K_C$	0.7935(3)	0.7266(2)	0.2640(2)	0.2542(2)	0.1354(10)	0.1327(4)	0.48680
$k_B T_c / J$	1.2602(5)	1.376(4)	3.788(2)	3.934(3)	7.39(5)	7.54(2)	
$k_B T_c / \tilde{J}$	1.6803(6)	1.8350(5)	1.894(1)	1.967(1)	1.97(1)	2.009(6)	2.0542
$C_0$	1.15(2)	1.10(3)	0.98(1)	0.94(1)			0.794



**Table 7.** Estimates of the secondary singularity, at  $-K_N$  for the uniform susceptibility and at  $-K_C$  for the staggered susceptibility, for the  $S = \frac{1}{2}$  models on the BCC lattice.

$[N, D]$	$F(K)$		$F_s(K)$	
	$K_C = 0.7936$	$\gamma = 1.416$	$K_C = 0.7266$	$\gamma = 1.435$
	$-K_N(\text{est.})$	residue	$-K_C(\text{est.})$	residue
[5, 7]	-0.7160	0.250	-0.7993	0.262
[6, 6]	-0.7159	0.250	-0.7985	0.260
[7, 5]	-0.7392	0.321	-0.8069	0.284
[5, 6]	-0.7189	0.254	-0.7987	0.261
[6, 5]	*		-0.7988	0.261
[4, 6]	-0.7111	0.242	-0.7994	0.262
[5, 5]	-0.7107	0.241	-0.7985	0.266
[6, 4]	-0.7244	0.275	-0.7911	0.241

**Figure 1.** Ratio plots for the uniform and staggered susceptibilities for the SC and BCC lattices (as indicated) for  $S = \frac{1}{2}, 1, \infty$ . The ratios are defined for the series in the variables  $\tilde{K} = JS(S+1)/k_B T$ , or equivalently  $r_n = a_n/(S(S+1)a_{n-1})$  where  $a_n$  are the coefficients of the  $K$ -series (2).

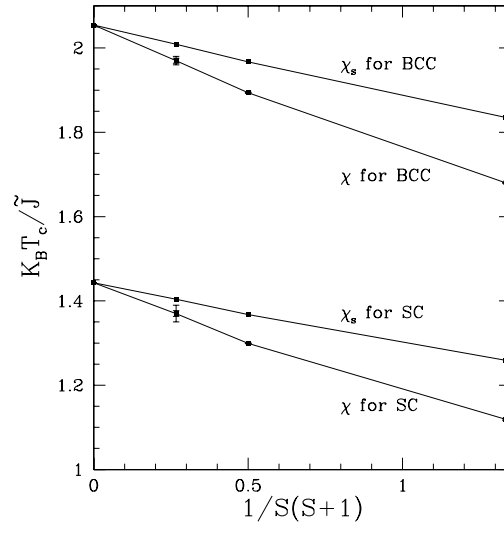


**Figure 2.**  $k_B T_c / J$  versus  $1/S(S+1)$ .